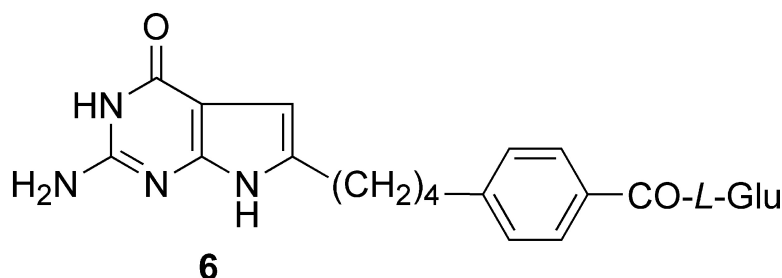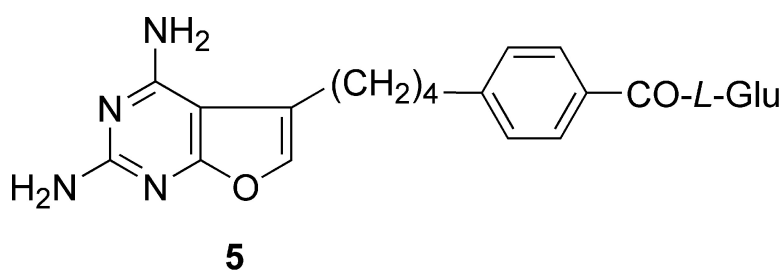Article

Synthesis of Classical, Four-Carbon Bridged 5-Substituted Furo[2,3-*d*]pyrimidine and 6-Substituted Pyrrolo[2,3-*d*]pyrimidine Analogues as Antifolates

Aleem Gangjee, Yibin Zeng, John J. McGuire, and Roy L. Kisliuk

More About This Article

Additional resources and features associated with this article are available within the HTML version:

- Supporting Information
- Links to the 5 articles that cite this article, as of the time of this article download
- Access to high resolution figures
- Links to articles and content related to this article
- Copyright permission to reproduce figures and/or text from this article

View the Full Text HTML

Synthesis of Classical, Four-Carbon Bridged 5-Substituted Furo[2,3-*d*]pyrimidine and 6-Substituted Pyrrolo[2,3-*d*]pyrimidine Analogues as Antifolates[1]

Aleem Gangjee,*,[†] Yibin Zeng,[†,#] John J. McGuire,[‡] and Roy L. Kisliuk[§]

Division of Medicinal Chemistry, Graduate School of Pharmaceutical Sciences, Duquesne University, Pittsburgh, Pennsylvania 15282, Grace Cancer Drug Center, Roswell Park Cancer Institute, Elm and Carlton Streets, Buffalo, New York 14263, and Department of Biochemistry, Tufts University School of Medicine, Boston, Massachusetts 02111

We report, for the first time, the biological activities of four-carbon-atom bridged classical antifolates on dihydrofolate reductase (DHFR), thymidylate synthase (TS), and folylpolyglutamate synthetase (FPGS) as well as antitumor activity. Extension of the bridge homologation studies of classical two-carbon bridged antifolates, a 5-substituted 2,4-diaminofuro[2,3-*d*]pyrimidine (**1**) and a 6-substituted 2-amino-4-oxopyrrolo[2,3-*d*]pyrimidine (**2**), afforded two four-carbon bridged antifolates, analogues **5** and **6**, with enhanced FPGS substrate activity and inhibitory activity against tumor cells in culture (EC$_{50}$ ≤ 10^{-7} M) compared with the two-carbon bridged analogues. These results support our original hypothesis that the distance and orientation of the side chain *p*-aminobenzoyl-L-glutamate moiety with respect to the pyrimidine ring are a crucial determinant of biological activity. In addition, this study demonstrates that, for classical antifolates that are substrates for FPGS, poor inhibitory activity against isolated target enzymes is not necessarily a predictor of a lack of antitumor activity.

Introduction

Folate metabolism has long been recognized as an effective target for chemotherapy because of its crucial role in the biosynthesis of nucleic acid precursors.[2] Inhibitors of folate-dependent enzymes in cancer, microbial, and protozoan cells provide compounds that have found clinical utility as antitumor, antimicrobial, and antiprotozoal agents.[3,4]

Variations in the atoms that link the heterocycle to the *p*-aminobenzoyl-L-glutamate of classical antifolates have been a particularly fruitful area of modification.[2−4] Methotrexate (MTX) and the recently approved pemetrexed (LY231514) (Figure 1) are both clinically used antitumor agents and have variations in the "bridge region"[2−4] different from that of folic acid. MTX contains a CH$_2$−N(CH$_3$) bridge, while pemetrexed contains a two-carbon atom bridge. A vast number of linkers have been used that involve replacing the −CH$_2$−NH− bridge of folic acid with carbon and heteroatoms as well as homologation to three atom bridges.[2−4] However, a search of the literature indicates that there is a paucity of information on extending the bridge to a four-atom chain. The only two examples available are of the synthesis of bishomofolic acid reported in 1967[5] with a CH$_2$CH$_2$CH$_2$NH bridge and a four-carbon-atom bridged analogue.[6] However, no biological activity of either compound was or has been reported in the literature. Thus, there are no reports in the literature on the biological activities of antifolates with a four-atom

bridge between the heterocycle and the *p*-aminobenzoyl-L-glutamate portion. This lack of information is surprising given the vast literature on classical antifolates and the remarkable activity of three-carbon-atom bridged analogues.[7] This study is the first report, to our knowledge, of the biological activities of classical antifolates with a four-carbon atom bridge.

As part of a continuing effort to develop novel classical antifolates as dihydrofolate reductase (DHFR) inhibitors and as antitumor agents, Gangjee et al.[8] previously reported the synthesis of *N*-[4-[2-(2,4-diaminofuro[2,3-*d*]pyrimidin-5-yl)ethyl]benzoyl]-L-glutamic acid (**1**) as a novel 6−5 bicyclic antifolate, which is reasonably potent against the growth of tumor cells in culture (EC$_{50}$ = 10^{-7}−10^{-8} M). We have recently demonstrated that a simple homologation of the C8−C9 bridge region to a three-carbon bridge, analogue **3**, enhances the antitumor activity (EC$_{50}$ = 10^{-8}−10^{-9} M).[9] It was therefore of interest to further explore the bridge homologation strategy to study the optimal bridge length requirement for classical 5-substituted furo[2,3-*d*]pyrimidines for enzyme inhibitory activity and antitumor activity and also to provide information on the biological and antitumor effects of a four-carbon-atom bridge in classical antifolates. Thus, compound **5**, *N*-[4-[4-(2,4-diaminofuro-[2,3-*d*]pyrimidin-5-yl)butyl]benzoyl]-L-glutamic acid, a four-carbon bridged analogue, was designed and synthesized.

Pemetrexed, a multitarget antifolate recently approved as an antitumor agent, is reported to be a dual thymidylate synthase (TS)−DHFR inhibitor (hTS K_i = 340 nM; hDHFR K_i = 7 nM).[10] The 6-regio isomer of pemetrexed, compound **2**, reported by Taylor et al.[11] was, however, inactive against the growth of tumor cells in culture. A possible reason for its inactivity in culture

* To whom correspondence should be addressed. Phone: (412) 396-6070. Fax: (412) 396-5593. E-mail: gangjee@duq.edu.
† Duquesne University.
# Current address: Department of Medicinal Chemistry, The University of Kansas, Lawrence, KS 66045.
‡ Roswell Park Cancer Institute.
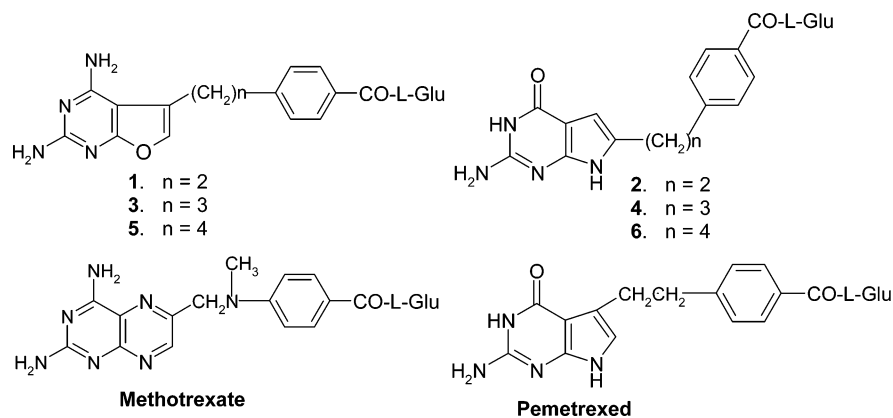§ Tufts University School of Medicine.

Figure 1.

could be that transposing the 5-ethylene bridge to the 6-position forces the benzoylglutamic acid side chain in an orientation different from that required for optimal enzyme interaction and antitumor activity. We speculated that elongation of the ethylene bridge of **2** would allow greater conformational flexibility and could perhaps restore the inhibitory activity against the growth of tumor cells in culture. Gangjee et al.[9] recently described a three-carbon bridged analogue of **2**, compound **4**, which had enhanced antitumor activity in culture. Thus, compound **6**, *N*-[4-[4-(2-amino-3,4-dihydro-4-oxo-7*H*-pyrrolo[2,3-*d*]pyrimidin-6-yl)butyl]benzoyl]-L-glutamic acid was also synthesized to explore further the bridge length potential for antitumor activity.

Polyglutamylation via folylpolyglutamate synthetase (FPGS) is an important mechanism for trapping classical folates and antifolates within the cell, thus maintaining high intracellular concentrations and in some instances for increasing binding affinity to folate-dependent enzymes and antitumor activity.[12,13] The enhanced antitumor activities of analogues **3** and **4** were attributed, in part, to their increased efficiency as human FPGS substrates compared to their two-carbon bridged parent analogues **1** and **2**, respectively. Thus, it was also of interest to determine the optimal bridge length requirement of the classical 5-substituted 2,4-diaminofuro[2,3-*d*]pyrimidine and 6-substituted 2-amino-4-oxoprrolo[2,3-*d*]pyrimidine with respect to human FPGS activity.

Chemistry

Compounds **5** and **6** were obtained via a nine-step synthesis from the commercially available methyl 4-formylbenzoate (**7**) using an α-chloromethyl ketone condensation with pyrimidine as the key step as outlined in Schemes 1 and 2. Thus, a Wittig reaction[14] of **7** with 3-(4-carbomethoxyphenyl)propyltriphenylphosphonium bromide **8** in 1:1 DMSO/THF with 2 equiv of NaH in an ice bath and N₂ atmosphere afforded the penten-4-enoic acid **9** as a mixture of *E*- and *Z*-isomers (Scheme 1). Hydrogenation of **9** afforded the pentanoic acid **10**, which was converted to the acid chloride **11** and immediately reacted with diazomethane followed by concentrated HCl to give the desired α-chloroketone **12**.[15]

With the desired α-chloroketone **12** in hand, the next step was the condensation of 2,4-diamino-6-hydroxypyrimidine **13** with **12** (Scheme 2). When DMF was used

Scheme 1
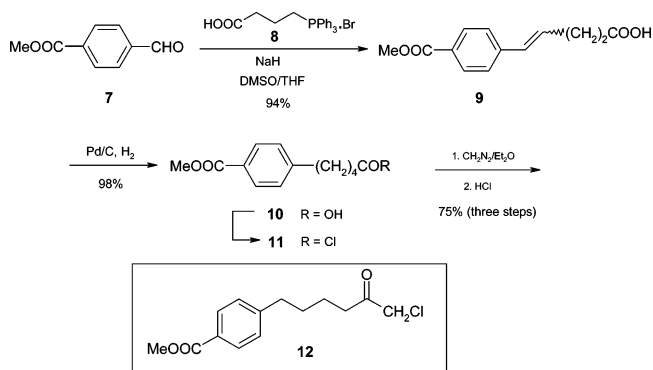
Scheme 2
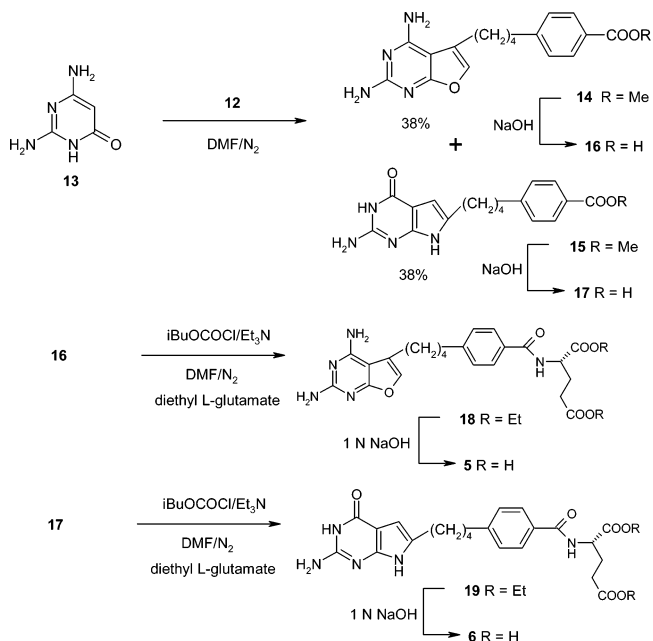
as solvent at room temperature for 24 h, compound **14** was obtained in 10% yield along with the recovery of starting materials. Increasing the reaction temperature and time afforded both the furo[2,3-*d*]pyrimidine **14** and pyrrolo[2,3-*d*]pyrimidine **15**. Optimal yields were obtained at 40–45 °C for 3 days, and **14** and **15** were each isolated, after chromatographic separation, in 38% yield (76% total). Hydrolysis of **14** and **15** afforded the corresponding free acids **16** and **17**. Subsequent coupling with L-glutamate diethyl ester using isobutyl chlorofor-

Table 1. Inhibitory Concentration (IC_{50} in μM) against Isolated DHFR and TS[a]

	DHFR			TS		
	rh	*E. coli*	*L. casei*	rh	*E. coli*	*L. casei*
1[b]	1.0	ND[d]	0.1	220	ND[d]	ND[d]
3[c]	9.0	7.0	10	>18	>180	>100
4[c]	>21 (16%)	22	>110	>17	>180	>100
5	21	21	10	>18	>100	>100
6	>20	100	>110	>17	>170	>100
MTX	0.022	0.007	0.022	ND[d]	ND[d]	ND[d]
PDDF	ND[d]	ND[d]	ND[d]	0.18	0.09	0.009
pemetrexed	2.3	230	230	19	38	38

[a] The percent inhibition was determined at a minimum of four inhibitor concentrations within 20% of the 50% point. The standard deviations for determination of 50% points were within ±10% of the value given. Recombinant human (rh) DHFR was kindly provided by Dr. J. H. Freisheim, Medical College of Ohio, Toledo, OH. *E. coli* DHFR was kindly provided by Dr. R. L. Blakley, St. Jude Children's Research Hospital, Memphis, TN. Recombinant human (rh) TS and *E. coli* TS was kindly provided by Dr. Frank Maley, New York State Department of Health, Albany, NY. PDDF was kindly provided by Dr. M. G. Nair, University of South Alabama, Mobile, AL. Pemetrexed was kindly provided by Dr. Chuan Shih, Eli Lilly and Co., Indianapolis, IN. [b] Data derived from ref 8. [c] Data derived from ref 9. [d] ND = not determined.

mate as the activating agent[12] afforded the diesters **18** and **19**. Final saponification of the diesters gave the target compounds **5** and **6**.

Biological Evaluation and Discussion

DHFR and TS Inhibition. Compounds **5** and **6** were evaluated as inhibitors of *Escherichia coli* (ec), *Lactobacillus casei* (lc), and recombinant human (rh) DHFR.[15] The inhibitory potency (IC_{50}) values are listed in Table 1 and compared with the values for MTX, **3**, and **4** and the previously reported values for **1**.[8] Both compounds **5** and **6** were poorly active against DHFR with IC_{50} values greater than 10^{-5} M.

Analogues **5** and **6** were also evaluated as inhibitors of ecTS, lcTS, and rhTS[12,13] and compared to pemetrexed and PDDF, a standard TS inhibitor, as a control. Both analogues **5** and **6** were inactive at the highest concentration tested (Table 1).

In Vitro Human Tumor Cell Growth Inhibition. Growth inhibitory potency of analogues **5** and **6** were compared to that of MTX in continuous exposure against the CCRF-CEM human lymphoblastic leukemia[16] and a series of MTX-resistant sublines[17–19] (Table 2). Compound **6** was about 85-fold less potent than MTX, while **5** was only 9-fold less potent than MTX. DHFR overexpressing line R1 was less than 3-fold cross-resistant to **6**, suggesting that DHFR is probably not the primary target of this analogue. In contrast, R1 was greater than 40-fold cross-resistant to **5**, suggesting that it primarily inhibits DHFR, as expected on the basis of its 2,4-diaminofuropyrimidine structure. The MTX-resistant transport-deficient subline R2, which does not express functional reduced folate carrier (RFC),[20] is 7-fold cross-resistant to **6** and 2-fold cross-resistant to **5**, while it is 115-fold resistant to MTX. The data suggest that **6** utilizes the RFC as its primary means of transport, but at high extracellular levels it is able to diffuse through the plasma membrane. The data also suggest that an alternative carrier may transport **5** in CCRF-CEM cells. A subline (R30dm) expressing low levels of FPGS is highly cross-resistant to both analogues under continu-

Table 2. Growth Inhibition of Parental CCRF-CEM Human Leukemia Cells and Sublines with Single, Defined Mechanisms of MTX Resistance during Continuous (0–120 h) Exposure to MTX, **5**, or **6**[a]

	EC_{50}, nM			
drug	CCRF-CEM	R1[b] (↑ DHFR)	R2[c] (↓ uptake)	R30dm[d] (↑ Glu$_n$)
MTX	13.0 ± 0	620 ± 40	1500 ± 0	14.5 ± 0.5
1[e]	290 ± 10	4250 ± 50	ND[f]	ND[f]
3[g]	60 ± 14	≥4600	1050 ± 50	84 ± 8
4[g]	460 ± 10	860 ± 150	4350 ± 650	470 ± 60
5	120 ± 10	4850 ± 950	265 ± 25	3150 ± 150
6	1100 ± 100	3050 ± 150	8100 ± 400	18000[h]

[a] Values presented are the average ± range for $n = 2$. [b] CCRF-CEM subline resistant to MTX solely as a result of a 20-fold increase in wild-type DHFR protein and activity.[14] [c] CCRF-CEM subline resistant as a result of decreased uptake of MTX.[15] [d] CCRF-CEM subline resistant to MTX solely as a result of decreased polyglutamylation. This cell line has 1% of the FPGS specific activity (measured with MTX as the folate substrate) of parental CCRF-CEM.[16] [e] Data derived from ref 8. [f] ND = not determined. [g] Data from ref 9. [h] The first experiment with this line indicated an EC_{50} greater than 10 000 nM. The value presented is from a second experiment covering a higher range.

Table 3. Protection of CCRF-CEM Human Leukemia Cells against the Growth Inhibitory Effects of MTX, **5**, and **6** by 10 μM Hypoxanthine (Hx), 5 μM Thymidine (TdR), and Their Combination[a]

	relative growth,[b] %			
drug	no addition	5 μM TdR	10 μM Hx	Hx + TdR
MTX (30 nM)	14 ± 1	18 ± 1	17 ± 0	82 ± 2
6 (5000 nM)	21 ± 0	18 ± 1	85 ± 4	85 ± 1
MTX (30 nM)	13 ± 0	16 ± 0	16 ± 1	75 ± 7
5 (5000 nM)	20 ± 1	20 ± 0	21 ± 0	74 ± 2

[a] Growth is expressed relative to quadruplicate cultures not treated with either drug or metabolite and is the average ± range for duplicate treated samples. Each experiment was repeated for each drug with similar results. [b] Deoxycytidine (dCyd, 10 μM) was present in all the above cultures to prevent the inhibition of growth caused in T-cell leukemias like CCRF-CEM by TdR (see Experimental Section). In typical results, dCyd alone had no effect on CCRF-CEM growth (96 ± 2% of control) and did not protect against growth inhibition by any of these drugs (data not shown). Hx alone (98 ± 1% of control) or in the presence of dCyd (97 ± 1% of control) did not affect CCRF-CEM growth and did not protect against MTX-induced growth inhibition (table above). TdR alone inhibited growth of CCRF-CEM (35 ± 0% of control), but TdR + dCyd was essentially not growth-inhibitory (94 ± 0% of control) and was not protected against MTX-induced growth inhibition (table above). Similarly, Hx + TdR + dCyd did not appreciably inhibit growth of CCRF-CEM (93 ± 1% of control).

ous exposure conditions, suggesting that polyglutamate forms of these analogues are essential to their mechanisms of action. Both **5** and **6** had increased inhibitory potency against CCRF-CEM cell growth in culture compared to their two-carbon bridged parent analogues but were less potent than the corresponding three-carbon bridge analogues **3** and **4**. These data suggest that the three-carbon bridge may be optimal for the classical 5-substituted 2,4-diaminofuro[2,3-*d*]pyrimidine and 6-substituted 2-amino-4-oxopyrrolo[2,3-*d*]pyrimidine with respect to antitumor activity.

Metabolite protection studies (Table 3) were performed to further elucidate the mechanism of action of **5** and **6**. At concentrations of drug that inhibited growth of CCRF-CEM cells by ≥90%, leucovorin was able to fully protect against the effects of MTX, **6**, and **5** (data not shown). This is consistent with an antifolate mechanism of action for both drugs. Further studies in CCRF-

Table 4. Activity of **5** and **6** as Substrates for Recombinant Human FPGS[a]

substrate	K_m, μM	$V_{max,rel}$	$V_{max,rel}/K_m$	n
AMT	5.4 ± 0.8	1.00	0.19	7
1[c]	8.5 ± 17	0.65 ± 0.01	0.07	2
3[d]	0.3 ± 0	0.42 ± 0.02	1.4	2
4[d]	0.9 ± 0.01	0.57 ± 0.06	0.63	3
5	2.0 ± 0.4	0.54 ± 0.02	0.27	3
6	6.3 ± 0.4	0.54 ± 0.02	0.086	3

[a] FPGS substrate activity was determined as described in Experimental Section at 2 mM L-[^{3}H]glutamate. Values presented are the average $\pm$ SD. [b] $V_{max,rel}$ is calculated on the basis of the apparent V_{max} of a substrate relative to the apparent V_{max} of AMT within the same experiment. [c] Data derived from ref 8. [d] Data from ref 9.

CEM cells examined the ability of thymidine (TdR) and/or hypoxanthine (Hx) to protect against growth inhibition. These metabolites can be salvaged to produce dTTP and the purine dNTPs required for DNA synthesis and thus bypass the MTX blockade.[21] As described in the Experimental Section, in T-lymphoblast cell lines such as CCRF-CEM, TdR can only be tested in the presence of dCyd, which reverses its toxic effects; however, dCyd has no protective effect on MTX either alone or in paired combination with either Hx or TdR (Table 3; footnote). The data (Table 3) show that for **6**, Hx alone could protect against growth inhibition, and addition of other metabolites did not improve the protection. These data suggest that **6** inhibits purine synthesis only; this is also consistent with the low level of cross-resistance of the DHFR overproducing the R1 subline (above). Since there are two folate-dependent formyltransferases in purine synthesis (i.e., GAR formyltransferase and AICAR formyltransferase), it would be of interest to know which is inhibited. Current anti-purine antifolates are primarily targeted to GAR formyltransferase.[22] For **5**, neither TdR nor Hx alone protected to any significant extent; both metabolites were required to achieve significant protection. This indicates that both purine and thymidylate synthesis are inhibited and is consistent with DHFR being the primary target of **5**.

FPGS Substrate Activity. The cross-resistance data for FPGS-deficient subline R30dm (above) suggest that **5** and **6** must be substrates for human FPGS. Their activity was evaluated in vitro with recombinant human FPGS and compared to that of aminopterin (AMT), a good substrate for FPGS. The data (Table 4) show that both **5** and **6** are substrates for human FPGS. Compound **6** was only half as efficient as AMT primarily because of its decreased V_{max}, while compound **5** was slightly more efficient than AMT. These results suggest that metabolism to polyglutamates must be considered in the mechanism of action of both **5** and **6**. Elongation of the bridge region in the series of 2-amino-4-oxopyrrolo[2,3-*d*]pyrimidines, of which **6** is a member, showed interesting effects on biological properties. This series shows dramatic changes in V_{max} as well as in K_m for FPGS activity. The three-carbon-bridge compound **4** has a very low K_m (0.9 μM) and a $V_{max,rel}$ of 0.57. Increasing the length of the bridge to four carbons in **6** described here caused an increase in K_m of 7-fold with no effect on V_{max}. Growth inhibitory potency against CCRF-CEM also shows an optimum at three carbons in this series. Interestingly, for the compounds in this series that were potent enough to perform metabolite protection (i.e.,

Table 5. Cytotoxicity Evaluation (GI$_{50}$, M) of Compounds **5** and **6** against Selected Tumor Cell Lines[23]

cell lines	compound **5**	compound **6**
leukemia		
HL-60(TB)	3.81×10^{-8}	6.56×10^{-6}
SR	4.78×10^{-8}	6.09×10^{-7}
K-562	2.14×10^{-7}	3.98×10^{-7}
colon cancer		
SW-620	7.83×10^{-8}	3.81×10^{-6}
renal cancer		
786-0	$>1.0 \times 10^{-4}$	8.98×10^{-7}

three- and four-carbon bridged), the data suggest that they are both inhibitors of de novo purine synthesis. The high degree of cross-resistance of the FPGS-deficient subline to the homologue **6** suggests that polyglutamylation is required even in continuous exposure.

Elongation of the bridge region in the series of substituted 2,4-diaminofuro[2,3-*d*]pyrimidines, of which **5** is a member, also has interesting effects on biological activity. In contrast to the 2-amino-4-oxopyrrolo[2,3-*d*]-pyrimidines, as the bridge is homologated from two to four carbons, the $V_{max,rel}$ for human FPGS substrate activity remains relatively constant; however, the K_m values vary widely without a consistent pattern. Compound **3** has the lowest K_m (0.3 μM) and is the most efficient FPGS substrate in this group. The other chain lengths each have similar growth inhibitory potencies, but the three-carbon bridged compound **3** is the most potent in this series. The two-carbon through four-carbon bridged homologues all appear to be DHFR inhibitors based on their metabolite protection profiles, as expected from their 2,4-diamino substituents.

Cytotoxicity Assays. Compounds **5** and **6** were selected by the National Cancer Institute[23] for evaluation of its in vitro preclinical antitumor screening program. The ability of compounds **5** and **6** to inhibit the growth of the sixty tumor cell lines of the NCI was evaluated. The data for selected tumor cell lines measured as GI$_{50}$ values, the concentration required to inhibit the growth of tumor cells in culture by 50% compared to a control, are reported in Table 5. Interestingly, compound **5** was a potent inhibitor against the growth of several tumor cell lines in culture, with GI$_{50}$ values in the 10^{-8} M range (HL-60, SR, SW-620) (Table 5), and compound **6** also had moderate inhibitory activity against several tumor cell lines with GI$_{50}$ values in the $10^{-6}-10^{-7}$ M range (Table 5). The compounds were relatively inactive (GI$_{50}$ < 10^{-6} M) against other tumor cell lines, indicating that these analogues are not general cell poisons but afford selective inhibition of some tumor cell lines. These data suggest that elongation of the bridge length from a two-carbon to a three- or four-carbon bridge in the classical 5-substituted 2,4-diaminofuro[2,3-*d*]pyrimidine and 6-substituted 2-amino-4-oxopyrrolo[2,3-*d*]pyrimidine is conducive to the inhibition of the growth of tumor cells in culture, with the three-carbon bridge being the most potent.

In summary, compound **5**, *N*-[4-[4-(2,4-diaminofuro-[2,3-*d*]pyrimidin-5-yl)butyl]benzoyl]-L-glutamic acid, and compound **6**, *N*-[4-[4-(2-amino-3,4-dihydro-4-oxo-7*H*-pyrrolo[2,3-*d*]pyrimidin-6-yl)butyl]benzoyl]-L-glutamic acid, were designed and synthesized to explore, for the first time, the biological effect of a four-carbon bridge of classical antifolates on DHFR and TS inhibitory

activity, FPGS substrate efficiency, and antitumor activity. Despite their poor inhibitory activity in isolated enzyme assays, both analogues **5** and **6** had better antitumor activity compared to the corresponding two-carbon-bridge analogues **1** and **2**, respectively, in tumor cell culture. Further, both **5** and **6** are good substrates for FPGS, which may account in part for their antitumor activities. These data suggest that the elongation to a four-carbon bridge of the two-carbon C8−C9 bridge of classical 5-substituted 2,4-diaminofuro[2,3-*d*]pyrimidines and 6-substituted 2-amino-4-oxopyrrolo[2,3-*d*]-pyrimidines is highly conducive to FPGS substrate activity and tumor inhibitory activity. The differential activities of the two-, three-, and four-carbon-atom bridges support our original hypothesis that the distance and orientation of the side chain *p*-benzoyl-L-glutamate moiety with respect to the pyrimidine ring are crucial determinants of the biological activities. In this series the three- and four-carbon bridges are better than the two-carbon bridge and the three-carbon bridge is optimal. These results also substantiate that for classical antifolates that are substrates for FPGS, poor activity against isolated target enzymes is not necessarily a predictor of a lack of antitumor activity.

Experimental Section

All evaporations were carried out in vacuo with a rotary evaporator. Analytical samples were dried in vacuo (0.2 mmHg) in a CHEM-DRY drying apparatus over P_2O_5 at 80 °C. Melting points were determined on a MEL-TEMP II melting point apparatus with FLUKE 51 K/J electronic thermometer and are uncorrected. Nuclear magnetic resonance spectra for proton (^{1}H NMR) were recorded on a Bruker WH-300 (300 MHz) spectrometer. The chemical shift values are expressed in ppm (parts per million) relative to tetramethyl-silane as internal standard: s = singlet, d = doublet, t = triplet, q = quartet, m = mutiplet, br = broad singlet. The relative integrals of peak areas agreed with those expected for the assigned structures. Thin-layer chromatography (TLC) was performed on POLYGRAM Sil G/UV254 silica gel plates with fluorescent indicator, and the spots were visualized under 254 and 366 nm illumination. Proportions of solvents used for TLC are by volume. Column chromatography was performed on 230−400 mesh silica gel purchased from Aldrich, Milwaukee, WI. Elemental analyses were performed by Atlantic Microlab, Inc. Norcross, GA. Element compositions are within ±0.4% of the calculated values. Fractional moles of water or organic solvents frequently found in some analytical samples of antifolates could not be prevented despite 24−48 h of drying in vacuo and were confirmed where possible by their presence in the ^{1}H NMR spectra. All solvents and chemicals were purchased from Aldrich Chemical Co. or from Fisher Scientific and were used as received.

(*E*/*Z*)-5-(4′-Carbomethoxyphenyl)-4-pentenoic Acid (9). To a suspension of methyl 4-formylbenzoate (**7**) (3.2 g, 20 mmol) and (3-carboxypropyl)triphenylphosphonium bromide **8** (8.6 g, 20 mmol) in 80 mL DMSO/THF (1:1) was added 2 equiv of NaH (92%) (1.0 g, 40 mmol) in one portion in an ice bath and N_2 atmosphere. The resulting suspension was stirred in an ice bath for an additional 30 min and slowly warmed to room temperature for another 6 h. TLC indicated the disappearance of the aldehyde spot and formation of two spots centered at R_f = 0.19 (hexane/EtOAc, 3:1). To the reaction mixture cooled in an ice bath was added ice/water (100 g) followed by concentrated HCl (10 mL). The resulting solution was extracted with ether (100 mL × 3) and dried over Na_2SO_4. After evaporation of solvent, the residue was loaded on a silica gel column (4 × 20 cm) and flash-chromatographed with hexane/EtOAc (2:1) and the desired fractions were pooled. After evaporation of solvent the residue was recrystallized

from ethyl ether to afford 4.4 g (94%) of **9** as white crystals: mp 118−121 °C. ^{1}H NMR (DMSO-d_6) δ 2.21−2.30 (m, 4 H, CH_2−CH_2−COOH), 6.1−6.6 (m, 2 H, −CH=CH−), 7.30−7.32 (d, 2 H, C_6H_4), 7.75−7.77 (d, 2 H, C_6H_4), 11.58 (s, 1H, COOH). Anal. ($C_{13}H_{14}O_4$) C, H.

5-(4′-Carbomethoxyphenyl)pentanoic Acid (10). To a solution of **9** (3 g, 15 mmol) in EtOAc/CHCl₃ (2:1, 50 mL) was added 10% Pd/C (500 mg). The resulting suspension was hydrogenated in a Parr apparatus overnight at 45−50 psi hydrogen pressure. TLC indicated the disappearance of the starting material and the formation of one major spot at R_f = 0.29 (hexane/EtOAc, 3:1). The reaction mixture was filtered through Celite and washed with methanol (30 mL). After evaporation of the solvent, the residue was loaded on to a silica gel column (4 × 20 cm) and flash-chromatographed with hexane/EtOAc (3:1) and the desired fractions were pooled. After evaporation of the solvent and recrystallization from Et₂O/EtOAc (2:1), 3 g (98%) of **10** was obtained as white crystals: mp 86.9−88.5 °C; ^{1}H NMR (DMSO-d_6) δ 1.47−1.61 (m, 4 H, β-CH_2 and γ-CH_2), 2.20−2.51 (t, 2 H, α-CH_2), 2.62−2.67 (t, 2 H, benzylic-CH_2), 3.82 (s, 3 H, OMe), 7.32−7.34 (d, 2 H, C_6H_4), 7.86−7.88 (d, 2 H, C_6H_4), 12.11 (s, 1H, COOH). Anal. ($C_{13}H_{16}O_4$) C, H.

Chloromethyl (4′-Carbomethoxyphenyl)butyl Ketone (12). To a solution of 5-(4′-carbomethoxyphenyl)pentanoic acid (**10**) (2.4 g, 10 mmol) in a 100 mL flask was added oxalyl chloride (5 mL) and anhydrous CH_2Cl_2 (10 mL). The resulting solution was refluxed for 1 h and then cooled to room temperature. After evaporation of solvent under reduced pressure, the residue was dissolved in ethyl ether (20 mL). The resulting solution was added dropwise to an ice-cooled ether solution of diazomethane (generated in situ from 15 g *N*-nitroso-*N*-methylurea) over 10 min. To this solution was added concentrated HCl (20 mL). The resulting mixture was refluxed for 1.5 h. After the mixture was cooled to room temperature, the organic layer was separated and the aqueous layer was extracted with ethyl ether (100 mL × 2). The combined organic layers were washed with two portions of 10% Na_2CO_3 solution and dried over Na_2SO_4. The solvent was evaporated to afford 2 g (75%) of **12** as yellow needles: mp 74.6−75.6 °C; ^{1}H NMR (DMSO-d_6) δ 1.52−1.67 (m, 4 H, β-CH_2 and γ-CH_2), 2.51−2.56 (t, 2 H, α-CH_2), 2.59−2.64 (t, 2 H, benzylic CH_2), 3.82 (s, 3 H, OMe), 4.50 (s, 2 H, CH_2Cl), 7.33−7.35 (d, 2 H, C_6H_4), 7.86−7.88 (d, 2 H, C_6H_4). Anal. ($C_{14}H_{17}O_3Cl$) C, H, Cl.

Methyl 4-[4-(2,4-Diaminofuro[2,3-*d*]pyrimidin-5-yl)butyl]benzoate (14) and Methyl 4-[4-(2-Amino-3,4-dihydro-4-oxo-7*H*-pyrrolo[2,3-*d*]pyrimidin-6-yl)butyl]benzoate (15). To a suspension of 2,4-diamino-6-hydroxypyrimidine (**13**) (0.8 g, 6 mmol) in anhydrous DMF (15 mL) was added **12** (1.6 g, 6 mmol). The resulting mixture was stirred under N_2 at 40−50 °C for 3 days. TLC showed the disappearance of starting materials and the formation of two major spots at R_f = 0.32 and R_f = 0.26 (CHCl₃/MeOH, 6:1). After evaporation of solvent, CH_3OH (20 mL) was added followed by silica gel (5 g). Evaporation of the solvent afforded a plug, which was loaded onto a silica gel column (3.5 cm × 15 cm) and eluted initially with CHCl₃ followed by 3% MeOH in CHCl₃ and then 4% MeOH in CHCl₃. Fractions showing R_f = 0.32 were pooled and evaporated, and the resulting solid was recrystallized from MeOH to afford 770 mg (38%) of **14** as white crystals: mp 225.2−226.7 °C; ^{1}H NMR (DMSO-d_6) δ 1.55−1.65 (m, 4 H, C9−CH_2 and C10−CH_2), 2.61−2.70 (m, 4 H, C11−CH_2 and C8−CH_2), 3.82 (s, 3 H, OMe), 5.97 (s, 2 H, 4-NH₂), 6.40 (s, 2 H, 2-NH₂), 7.08 (s, 1 H, C6−CH), 7.32−7.35 (d, 2 H, C_6H_4), 7.85−7.87 (d, 2 H, C_6H_4). Anal. ($C_{18}H_{20}N_4O_3$) C, H, N.

Fractions that showed an R_f = 0.26 were pooled and evaporated, and the resulting residue was recrystallized from MeOH to afford 770 mg (38%) of **15** as light-yellow crystals: mp 241.9−243.7 °C; ^{1}H NMR (DMSO-d_6) δ 1.58 (m, 4 H, C9−CH_2 and C10−CH_2), 2.49−2.66 (m, 4 H, C11−CH_2 and C8−CH_2), 3.82 (s, 3 H, OMe), 5.83 (s, 1 H, C5−CH), 5.96 (s, 2 H, 4-NH₂), 7.32−7.34 (d, 2 H, C_6H_4), 7.85−7.87 (d, 2 H, C_6H_4),

10.12 (s, 1 H, 3-NH), 10.80 (s, 1 H, 7-NH). Anal. (C$_{18}$H$_{20}$N$_4$O$_3$·0.1H$_2$O) C, H, N.

4-[4-(2,4-Diaminofuro[2,3-*d*]pyrimidin-5-yl)butyl]benzoic Acid (16). To a suspension of **15** (250 mg, 7 mmol) in CH$_3$OH/DMSO (1:1) was added 2 N NaOH (15 mL). The resulting mixture was stirred under N$_2$ at 40−50 °C for 5 h. TLC indicated the disappearance of starting material and the formation of one major spot at the origin. The resulting solution was passed through Celite and washed with a minimum amount of CH$_3$OH. The combined filtrate was evaporated under reduced pressure to dryness. To this residue was added distilled water (15 mL). The solution was cooled in an ice bath, and the pH was adjusted 3 to 4 using 2 N HCl. The resulting suspension was chilled in a dry ice/acetone bath and thawed to 4 °C overnight in a refrigerator. The precipitate was filtered, washed with cold water, and dried in a desiccator under reduced pressure using P$_2$O$_5$ to afford 230 mg (85%) of **16** as a light-yellow powder: mp >270 °C (dec); R_f = 0.30 (CHCl$_3$/MeOH, 5:1); ^{1}H NMR (DMSO-d_6) δ 1.54−1.66 (m, 4 H, C9−CH$_2$ and C10−CH$_2$), 2.67 (br, 4 H, C11−CH$_2$ and C8−CH$_2$), 7.30−7.40 (m, 5 H, NH$_2$, C6−CH, C$_6$H$_4$), 7.70 (s, 2 H, NH$_2$), 7.84−7.86 (d, 2 H, C$_6$H$_4$), 8.26 (s, 2 H, 2-NH2), 12.80 (s, 1 H, COOH). Anal. (C$_{17}$H$_{18}$N$_4$O$_3$·1.0HCl·0.60MeOH) C, H, N. This acid was used directly for the next step without further purification.

Diethyl *N*-{4-[4-(2,4-Diaminofuro[2,3-*d*]pyrimidin-5-yl)butyl]benzoyl}-L-glutamate (18). To a solution of **16** (175 mg, 0.45 mmol) in anhydrous DMF (9 mL) was added triethylamine (130 μL), and the mixture was stirred under N$_2$ at room temperature for 5 min. The resulting solution was cooled to 0 °C. Isobutyl chloroformate (130 μL, 1.5 mmol) was added, and the mixture was stirred at 0 °C for 30 min. At this time, TLC (MeOH/CHCl$_3$, 1:5) indicated the formation of the activated intermediate at R_f = 0.57 and the disappearance of the starting acid at R_f = 0.30. Diethyl l-glutamate hydrochloride (240 mg, 1.0 mmol) was added to the reaction mixture followed immediately by triethylamine (130 μL, 1.0 mmol). The reaction mixture was allowed to slowly warm to room temperature and stirred under N$_2$ for 18 h. The reaction mixture was then subjected to a second cycle of activation and coupling using half the quantities listed above. The reaction mixture was allowed to slowly warm to room temperature and stirred under N$_2$ for another 24 h. The reaction mixture was then evaporated to dryness under reduced pressure. The residue was dissolved in a minimum amount of CHCl$_3$/MeOH, 4:1, chromatographed on a silica gel column (2 cm × 15 cm), and eluted with 4% MeOH in CHCl$_3$. The desired fractions (TLC) were pooled, evaporated to dryness, and recrystallized from ethyl ether to afford 200 mg (85%) of **18** as yellow needles: mp 135.2−136.8 °C; R_f = 0.57 (MeOH/CHCl$_3$, 1:5); ^{1}H NMR (DMSO-d_6) δ 1.13−1.20 (m, 6 H, OEt), 1.56−1.66 (m, 4 H, C9−CH$_2$ and C10−CH$_2$), 1.99−2.11 (two sets of t, 2 H, Glu β-CH$_2$), 2.40−2.45 (t, 2 H, Glu γ-CH$_2$), 2.50−2.67 (m, 4 H, C11−CH$_2$, C8−CH$_2$), 4.00−4.13 (m, 4 H, OEt), 4.33−4.40 (m, 1 H, Glu α-CH), 5.94 (s, 2 H, 4-NH$_2$), 6.38 (s, 2 H, 2-NH$_2$), 7.08 (s, 1 H, C6−CH), 7.28−7.31 (d, 2 H, C$_6$H$_4$), 7.77−7.80 (d, 2 H, C$_6$H$_4$), 8.62−8.64 (d, 1 H, −CONH−). Anal. (C$_{26}$H$_{33}$N$_5$O$_6$) C, H, N.

***N*-{4-[4-(2,4-Diaminofuro[2,3-*d*]pyrimidin-5-yl)butyl]benzoyl}-L-glutamic Acid (5).** To a solution of the diester **18** (150 mg, 0.3 mmol) in MeOH (10 mL) was added 1 N NaOH (6 mL), and the mixture was stirred under N$_2$ at room temperature for 16 h. TLC showed the disappearance of the starting material (R_f = 0.62) and one major spot at the origin (MeOH/CHCl$_3$, 1:5). The reaction mixture was evaporated to dryness under reduced pressure. The residue was dissolved in water (10 mL). The resulting solution was cooled in an ice bath, and the pH was adjusted to 3−4 with dropwise addition of 1 N HCl. The resulting suspension was frozen in a dry ice/acetone bath and thawed in the refrigerator to 4−5 °C and filtered. The residue was washed with a small amount of cold water and ethyl acetate and dried in vacuo using P$_2$O$_5$ to afford 130 mg (92%) of **5** as a white powder: mp 163−165 °C; ^{1}H NMR (DMSO-d_6) δ 1.56−1.66 (m, 4 H, C9−CH$_2$ and C10−CH$_2$), 1.95−2.08 (m, 2 H, Glu β-CH$_2$), 2.32−2.35 (t, 2 H, Glu γ-CH$_2$), 2.50−2.66 (m, 4 H, C11−CH$_2$, C8−CH$_2$), 4.36−4.40 (br, 1 H, Glu α-CH), 5.80−5.95 (br, 2 H, 4-NH$_2$), 6.40 (s, 2 H, 2-NH$_2$), 7.20−7.50 (m, 3 H, C6−CH, C$_6$H$_4$), 7.79−7.82 (d, 2 H, C$_6$H$_4$), 8.52−8.55 (d, 1 H, −CONH−),12.38−12.53 (br, 2 H, 2 × COOH). Anal. (C$_{22}$H$_{25}$N$_5$O$_6$·1.4H$_2$O) C, H, N.

4-[4-(2-Amino-3,4-dihydro-4-oxo-7*H*-pyrrolo[2,3-*d*]pyrimidin-6-yl)butyl]benzoic Acid (17). To a suspension of **15** (250 mg, 7 mmol) in CH$_3$OH/DMSO (1:1, 40 mL) was added 3 N NaOH (15 mL). The resulting mixture was stirred under N$_2$ at 40−50 °C for 5 h. TLC indicated the disappearance of starting material and the formation of one major spot at the origin. The resulting solution was passed through Celite and washed with a minimum amount of MeOH. The combined filtrate was evaporated to dryness under reduced pressure. To this residue was added distilled water (15 mL). The solution was cooled in an ice bath, and the pH was adjusted to 3−4 using 2 N HCl. The resulting suspension was chilled in a dry ice/acetone bath and thawed to 4 °C overnight in a refrigerator. The precipitate was filtered, washed with cold water, and dried in a desiccator under reduced pressure using P$_2$O$_5$ to afford 260 mg (90%) of **17** as a brown powder: mp >266 °C (dec); R_f = 0.18 (CHCl$_3$/MeOH, 5:1); ^{1}H NMR (DMSO-d_6) δ 1.54−1.60 (br, 4 H, C9−CH$_2$ and C10−CH$_2$), 2.49−2.65 (m, 4 H, C11−CH$_2$, C8−CH$_2$), 5.91 (s, 1 H, C5−CH), 6.64 (br, 2 H, 2-NH$_2$), 7.29−7.31 (d, 2 H, C$_6$H$_4$), 7.83−7.85 (d, 2 H, C$_6$H$_4$), 10.71 (s, 1 H, 3-NH), 11.17 (s, 1 H, 7-NH), 12.75 (s, 1 H, COOH). Anal. (C$_{17}$H$_{18}$N$_4$O$_3$·1.0HCl) C, H, N. This acid was used directly for the next step without further purification.

***N*-{4-[4-(2-Amino-3,4-dihydro-4-oxo-7*H*-pyrrolo[2,3-*d*]pyrimidin-6-yl)butyl]benzoyl}-L-glutamic Acid (6).** To a solution of **17** (135 mg, 0.37 mmol) in anhydrous DMF (9 mL) was added triethylamine (130 μL), and the mixture was stirred under N$_2$ at room temperature for 5 min. The resulting solution was cooled to 0 °C. Isobutyl chloroformate (130 μL, 1.0 mmol) was added, and the mixture was stirred at 0 °C for 30 min. At this time TLC (MeOH/CHCl$_3$, 1:5) indicated the formation of the activated intermediate at R_f = 0.55 and the disappearance of the starting acid at R_f = 0.18. Diethyl L-glutamate hydrochloride (240 mg, 1.0 mmol) was added to the reaction mixture followed immediately by triethylamine (130 μL, 1.0 mmol). The reaction mixture was slowly allowed to warm to room temperature and stirred under N$_2$ for 18 h. The reaction mixture was then subjected to a second cycle of activation and coupling using half the quantities listed above. The reaction mixture was slowly allowed to warm to room temperature and stirred under N$_2$ for 24 h. TLC showed the formation of one major spot at R_f = 0.55 (MeOH/CHCl$_3$, 1:5). The reaction mixture was evaporated to dryness under reduced pressure. The residue was dissolved in a minimum amount of CHCl$_3$/MeOH, 4:1, and chromatographed on a silica gel column (2 cm × 15 cm) with 4% MeOH in CHCl$_3$ as the eluent. Fractions that showed the desired single spot at R_f = 0.55 were pooled and evaporated to dryness to afford **19** as a yellow syrup, which was used directly for the next step.

To a solution of the diester **19** in MeOH (10 mL) was added 1 N NaOH (6 mL), and the mixture was stirred under N$_2$ at room temperature for 16 h. TLC showed the disappearance of the starting material (R_f = 0.55) and formation of one major spot at the origin (MeOH/CHCl$_3$, 1:5). The reaction mixture was evaporated to dryness under reduced pressure. The residue was dissolved in water (10 mL), the resulting solution was cooled in an ice bath, and the pH was adjusted to 3−4 with dropwise addition of 1 N HCl. The resulting suspension was frozen in a dry ice/acetone bath, thawed in a refrigerator to 4−5 °C, and filtered. The residue was washed with a small amount of cold water and ethyl acetate and dried in vacuo using P$_2$O$_5$ to afford 130 mg (70%, two steps) of **6** as a yellow powder: mp 171−173 °C; ^{1}H NMR (DMSO-d_6) δ 1.58 (br, 4 H, C9−CH$_2$ and C10−CH$_2$), 1.94−2.06 (m, 2 H, Glu β-CH$_2$), 2.34−3.37 (t, 2 H, Glu γ-CH$_2$), 2.49−2.69 (m, 4 H, C11−CH$_2$, C8−CH$_2$), 4.39 (m, 1 H, Glu α-CH), 5.84 (s, 1 H, C5−CH), 5.99 (s, 2 H, 2-NH$_2$), 7.26−7.29 (d, 2 H, C$_6$H$_4$), 7.77−7.80 (d, 2 H, C$_6$H$_4$), 8.50−8.53 (d, 1 H, −CONH), 10.16 (s, 1 H, 3-NH), 10.79 (s, 1

H, 7-NH), 12.38−12.53 (br, 2 H, 2 × COOH). Anal. ($C_{22}H_{25}N_5O_6$· 1.0HCl·0.6H_2O) C, H, N, Cl.

Dihydrofolate Reductase (DHFR) Assay.[24] All DHFR enzymes were assayed spectrophotometrically in a solution containing 50 μM dihydrofolate, 80 μM NADPH, 0.05 M Tris-HCl, 0.001 M 2-mercaptoethanol, and 0.001 M EDTA at pH 7.4 and at 30 °C. The reaction was initiated with an amount of enzyme yielding a change in OD at 340 nm of 0.015/min.

Thymidylate Synthase (TS) Assay. TS was assayed spectrophotometrically at 30 °C and pH 7.4 in a mixture containing 0.1 M 2-mercaptoethanol, 0.0003 M (6*R*,*S*)-tetrahydrofolate, 0.012 M formaldehyde, 0.02 M MgCl$_2$, 0.001 M dUMP, 0.04 M Tris-HCl, and 0.000 75 M NaEDTA. This was the assay described by Wahba and Friedkin[25] except that the dUMP concentration was increased 25-fold according to the method of Davisson et al.[26] The reaction was initiated by the addition of an amount of enzyme, yielding a change in absorbance at 340 nm of 0.016/min in the absence of inhibitor.

Cell Lines and Methods for Measuring Growth Inhibitory Potency (Table 2). Drug solutions were standardized using extinction coefficients. Extinction coefficients were determined for **5** (pH 1, λ_{max} = 248 nm (23 300); pH 7, λ_{max} = 249 nm (22 500); pH 13, λ_{max} = 249 nm (22 200)) and for **6** (pH 1, λ_{max} = 229 nm (23 200); pH 7, λ_{max} = 250 nm (22 500); pH 13, λ_{max} = 248 nm (21 900)). Extinction coefficients for methotrexate (MTX), a gift of Immunex (Seattle, WA), were from the literature.[27] Aminopterin, hypoxanthine (Hx), thymidine (TdR), and deoxycytidine (dCyd) were purchased from Sigma Chemical Co. (St. Louis, MO). Calcium leucovorin (LV) was purchased from Schircks Laboratories (Jona, Switzerland). Other chemicals and reagents were reagent grade or higher.

Cell lines were verified to be negative for Mycoplasma contamination (Mycoplasma Plus PCR primers, Stratagene, La Jolla, CA). The human T-lymphoblastic leukemia cell line CCRF-CEM[16] and its MTX-resistant sublines R1,[17] R2,[18] and R30dm[19] were cultured as described.[19] R1 expresses 20-fold elevated levels of dihydrofolate reductase (DHFR), the target enzyme of MTX. R2 has dramatically reduced MTX uptake but normal levels of MTX-sensitive DHFR. R30dm expresses 1% of the folylpolyglutamate synthetase (FPGS) activity of CCRF-CEM and is resistant to short-term, but not continuous, MTX exposure; however, R30dm is cross-resistant in continuous exposure to antifolates that require polyglutamylation to form potent inhibitors. Growth inhibition of all cell lines by continuous drug exposure was assayed as described.[19,28] EC_{50} values (drug concentration effective at inhibiting cell growth by 50%) were determined visually from plots of percent growth relative to a solvent-treated control culture versus the logarithm of drug concentration.

Protection against growth inhibition of CCRF-CEM cells was assayed by including leucovorin ((6*R*,*S*)-5-formyltetrahydrofolate) at 0.1−10 μM with a concentration of drug previously determined to inhibit growth by 90−95%. The remainder of the assay was as described. Growth inhibition was measured relative to the appropriate leucovorin-treated control; leucovorin, even at 10 μM, caused no growth inhibition in the absence of drug, however.

Protection against growth inhibition of CCRF-CEM cells was also assayed by including Hx (10 μM), TdR (5 μM), or dCyd (10 μM) individually in pairs (Hx + dCyd, TdR + dCyd) or all together (Hx + TdR + dCyd) with concentrations of MTX, **5**, or **6** that would inhibit growth by ∼80% or more over a growth period of ∼72 h. The growth period was limited because after 72 h CCRF-CEM cells deplete TdR in the growth media and drug effects are no longer protected. dCyd is added only to alleviate the growth inhibitory effects of 5 μM TdR against CCRF-CEM cells.[29] Controls with metabolites alone (no drug) in the combinations described above (in duplicate), controls with drug alone with no metabolites (in duplicate), and untreated controls with neither drugs nor metabolites (in quadruplicate) were performed. Growth inhibition was measured as percent growth relative to untreated control cells (absence of drugs and metabolites).

Folylpolyglutamate Synthetase (FPGS) Purification and Assay. Recombinant human cytosolic FPGS was purified and assayed as described previously.[13] Both **5** (93% recovery) and **6** (89% recovery) were themselves nearly quantitatively recovered during the standard assay procedure, thus ensuring that their polyglutamate products would also be quantitatively recovered. A fourth milliliter of 0.1 N HCl (which recovers the polyglutamate products) was required to obtain these recoveries of each analogue; however, kinetics constants were determined by the hyperbolic curve fitting subroutine of SigmaPlot (Jandel) or Kaleidagraph (Synergy Software) using a ≥10-fold range of substrate concentration. Activity was linear with respect to time at the highest and lowest substrate concentrations tested for **6**; linearity could not be maintained as well with **5**, but the kinetics constants still represent good estimates. Assays contained ∼400 units of FPGS activity; 1 unit of FPGS catalyzes incorporation of 1 pmol of [^{3}H]glutamate/ h. Because the K_m value for **5** was low, assays to determine its kinetic constants were modified to include 2 mM L-[^{3}H]-glutamate instead of the standard 4 mM. The resulting lower background allowed quantitation at lower levels of product synthesis. The K_m value for AMT was the same whether 2 or 4 mM glutamate was used (data not shown).

Supporting Information Available: Analysis data for **5**, **6**, **9**, **10**, **12**, **14**−**16**, **21**, and **22**. This material is available free of charge via the Internet at http://pubs.acs.org.

References

(1) Presented in part at the 93rd National Meeting of the American Association for Cancer Research, San Francisco, CA, April 2002; Abstract 1204.

(2) Berman, E. M.; Werbel, L. M. The Renewed Potential for Folate Antagonists in Contemporary Cancer Chemotherapy. *J. Med. Chem.* **1991**, *34*, 479−485. Kisliuk, R. L. Deaza Analogues of Folic Acid as Antitumor Agents. *Curr. Pharm. Des.* **2003**, *9*, 2615−2625.

(3) Rosowsky, A. Chemistry and Biological Activity of Antifolates. In *Progress in Medicinal Chemistry*; Ellis, G. P., West, G. B., Eds.; Elsevier Science Publishers: Amsterdam, 1989; pp 1−252.

(4) Gangjee, A.; Elzein, E.; Kothare, M.; Vasudevan, A. Classical and Nonclassical Antifolates as Potential Antitumor, Antipneumocystis and Antitoxoplasma Agents. *Curr. Pharm. Des.* **1996**, *2*, 263−280.

(5) Mosher, C. W.; Acton, E. M.; Crews, O. P.; Goodman, L. Bishomofolic Acid. A New Synthesis of Folic Acid Analogues. *J. Org. Chem.* **1967**, *32*, 1452−1458.

(6) Miwa, T.; Hitaka, T.; Akimoto, H. A Novel Synthetic Approach to Pyrrolo[2,3-*d*]pyrimidine Antifolates. *J. Org. Chem.* **1993**, *58*, 1696−1701.

(7) Miwa, T.; Hitaka, T.; Akimoto, H.; Nomura, H. Novel Pyrrolo-[2,3-*d*]pyrimidine Antifolates: Synthesis and Antitumor Activities. *J. Med. Chem.* **1991**, *34*, 555−560.

(8) Gangjee, A.; Devraj, R.; McGuire, J. J.; Kisliuk, R. L. Effect of Bridge Region Variation on Antifolate and Antitumor Activity of Classical 5-Substituted 2,4-Diaminofuro[2,3-*d*]pyrimidines. *J. Med. Chem.* **1995**, *38*, 3798−3805.

(9) Gangjee, A.; Zeng, Y.; McGuire, J. J.; Kisliuk, R. L. Synthesis of Classical, Three-Carbon-Bridged 5-Substituted Furo[2,3-*d*]pyrimidine and 6-Substituted Pyrrolo[2,3-*d*]pyrimidine Analogues as Antifolates. *J. Med. Chem.* **2004**, *47*, 6893−6901.

(10) Taylor, E. C.; Kuhnt, D.; Shih, C.; Rinzel, S. M.; Grindey, G. B.; Barredo, J.; Lannatipour, M.; Moran, R. A Dideazatetrahydrofolate Analogue Lacking a Chiral Center at C6, *N*-[4-[2-(2-Amino-3,4-dihydro-4-oxo-7*H*-pyrrolo[2,3-*d*]pyrimidine-5-yl)ethyl]-benzoyl]-L-glutamic acid, Is an Inhibitor of Thymidylate Synthase. *J. Med. Chem.* **1992**, *35*, 4450−4454.

(11) Shih, C.; Barnett, C. J.; Grindey, G. B.; Pearce, H. L.; Engelhardt, J. A.; Todd, G. C.; Rinzel, S. M.; Worzalla, J. F.; Gossett, L. S.; Everson, T. P.; Wilson, T. M.; Kobierski, M. E.; Winter, M. A.; Moran, R. G.; Kuhnt, D.; Taylor, E. C. Structural Features That

Determine the Biological Activity of Pyrrolo[2,3-*d*]pyrimidine Based Antifolates. Presented at the 10th International Symposium, Chemistry and Biology of Pteridines and Folates, Orange Beach, AL, March 21−26, 1993; Abstract: F15.

(12) Gangjee, A.; Zeng, Y.; McGuire, J. J.; Kisliuk, R. L. Effect of C9-Methyl Substitution and C8−C9 Conformational Restriction on Antifolate and Antitumor Activity of Classical 5-Substituted 2,4-Diaminofuro[2,3-*d*]pyrimidines. *J. Med. Chem.* **2000**, *43*, 3125−3133.

(13) Gangjee, A.; Dubash, N. P.; Zeng, Y.; McGuire, J. J. Recent Advances in the Chemistry and Biology of Folypoly-γ-glutamate Synthetase Substrates and Inhibitors. *Curr. Med. Chem.: Anti-Cancer Agents* **2002**, *2*, 331−355.

(14) Salley, J. J.; Glennon, R. A. Studies on Simplified Ergoline Derivatives. A General Six-Step Synthesis of Phenyl-Substituted 4-Methyl-3,4,4a,5,6,10b-hexahydrobenzo-[*f*]quinolin-1-(2*H*)-one Analogues (1). *J. Heterocycl. Chem.* **1982**, *19*, 545.

(15) DeGraw, J. L.; Kisliuk, R. L.; Gaumont, Y.; Baugh, C. M.; Nair, M. G. Synthesis and Antifolate Activity of 10-Deazaaminopterin. *J. Med. Chem.* **1974**, *17*, 552−553.

(16) Foley, G. F.; Lazarus, H.; Farber, S.; Uzman, B. G.; Boone, B. A.; McCarthy, R. E. Continuous Culture of Lymphoblasts from Peripheral Blood of a Child with Acute Leukemia. *Cancer* **1965**, *18*, 522−529.

(17) Mini, E.; Srimatkandada, S.; Medina, W. D.; Moroson, B. A.; Carman, M. D.; Bertino, J. R. Molecular and Karyological Analysis of Methotrexate-Resistant and -Sensitive Human Leukemic CCRF-CEM Cells. *Cancer Res.* **1985**, *45*, 317−325.

(18) Rosowsky, A.; Lazarus, H.; Yuan, G. C.; Beltz, W. R.; Mangini, L.; Abelson, H. T.; Modest, E. J.; Frei, E., III. Effects of Methotrexate Esters and Other Lipophilic Antifolates on Methotrexate-Resistant Human Leukemic Lymphoblasts. *Biochem. Pharmacol.* **1980**, *29*, 648−652.

(19) McCloskey, D. E.; McGuire, J. J.; Russell, C. A.; Rowan, B. G.; Bertino, J. R.; Pizzorno, G.; Mini, E. Decreased Folylpoly-glutamate Synthetase Activity as a Mechanism of Methotrexate Resistance in CCRF-CEM Human Leukemia Sublines. *J. Biol. Chem.* **1991**, *266*, 6181−6187.

(20) Wong, S. C.; Zhang, L.; Witt, T. L.; Proefke, S. A.; Bhushan, A.; Matherly, L. H. Impaired Membrane Transport in Methotrexate-Resistant CCRF-CEM Cells Involves Early Translation Termination and Increased Turnover of a Mutant Reduced Folate Carrier. *J. Biol. Chem.* **1999**, *274*, 10388−10394.

(21) Hakala, M. T.; Taylor, E. The Ability of Purine and Thymidine Derivatives and of Glycine To Support the Growth of Mammalian Cells in Culture. *J. Biol. Chem.* **1959**, *234*, 126−128.

(22) McGuire, J. J. Anticancer Antifolates: Current Status and Future Directions. *Curr. Pharm. Des.* **2003**, *9*, 2593−2613.

(23) We thank the Developmental Therapeutics Program of the National Cancer Institute for performing the in vitro anticancer evaluation.

(24) Kisliuk, R. L.; Strumpf, D.; Gaumont, Y.; Leary, R. P.; Plante, L. Diastereoisomers of 5,10-Methylene-5,6,7,8-tetrahydropteroyl-D-glutamic Acid. *J. Med. Chem.* **1977**, *20*, 1531−1533.

(25) Wahba, A. J.; Friedkin, M. The Enzymatic Synthesis of Thymidylate. Early Steps in the Purification of Thymidylate Synthetase of *Escherichia coli. J. Biol. Chem.* **1962**, *237*, 3794−3801.

(26) Davisson, V. J.; Sirawaraporn, W.; Santi, D. V. Expression of Human Thymidylate Synthase in *Escherichia coli. J. Biol. Chem.* **1989**, *264*, 9145−9148.

(27) Blakley, R. L. *The Biochemistry of Folic Acid and Related Pteridines*; Elsevier: Amsterdam, 1969; p 569.

(28) McGuire, J. J.; Magee, K. J.; Russell, C. A.; Canestrari, J. M. Thymidylate Synthase as a Target for Growth Inhibition in Methotrexate-Sensitive and -Resistant Human Head and Neck Cancer and Leukemia Cell Lines. *Oncol. Res.* **1997**, *9*, 139−147.

(29) Grindey, G. B.; Wang, M. C.; Kinahan, J. J. Thymidine Induced Perturbations in Ribonucleoside and Deoxyribonucleoside Triphosphate Pools in Human Leukemic CCRF-CEM Cells. *Mol. Pharmacol.* **1979**, *16*, 601−606.